

University of Wisconsin - Madison

MADPH-96-936

UPR-0696T

UTEXAS-HEP-96-2

DOE-ER-40757-078

April 1996

Baryonic Z' connection of LEP $R_{b,c}$ data with Tevatron $(W, Z, \gamma)b\bar{b}$ events

V. Barger^{a)}, Kingman Cheung^{b)}, and Paul Langacker^{c)}

^{a)}*Dept. of Physics, University of Wisconsin, Madison, WI 53706*

^{b)}*Center for Particle Physics, University of Texas, Austin, TX 78712*

^{c)}*Dept. of Physics and Astronomy, University of Pennsylvania, Philadelphia PA 19104*

Abstract

The mixing of a new Z' boson with the Z significantly improves the fit to the LEP precision electroweak data, provided that the Z' couples mainly to quarks. If $M_{Z_2} < 200$ GeV, the s -channel Z_2 production and $(W, Z, \gamma)Z_2$ pair production cross sections at the Tevatron give an excess above QCD of $b\bar{b}$ and $(W, Z, \gamma)b\bar{b}$ events, respectively, with invariant mass $m(b\bar{b}) \approx M_{Z_2}$, which provide viable signals for detection of the Z_2 . The interference of the Z_2 with γ, Z_1 in $e^+e^- \rightarrow b\bar{b}(\bar{c}c)$ at LEP 1.5 energies is correlated with $R_b(R_c)$ and may be observable.

The Standard Model (SM) has long provided an excellent representation of particle interactions. Recently, however, possible indications of discrepancies with SM predictions have surfaced in LEP[1] data. The LEP measurements[1] of

$$R_{b(c)} = \Gamma(Z \rightarrow \bar{b}b(\bar{c}c))/\Gamma(Z \rightarrow \text{hadrons}) \quad (1)$$

deviate by 3.7σ (-2.4σ) from the SM[2,3].* These deviations have generated a flurry of phenomenological activity since they may be the first indications of physics beyond the SM. Proposed explanations of the observed phenomena include supersymmetric[5] or other new particles[6], extra Z bosons[7,8,9,10,11,12,13,14,15,16], technicolor[17], and other[18] models. Our interest here is in possible extra Z boson interpretations, which have immediate implications for physics at the Tevatron. We point out that s -channel Z_2 production and the pair production processes $(W, Z, \gamma)Z_2$ with $Z_2 \rightarrow \bar{b}b$ decays will lead to $\bar{b}b$ and $(W, Z, \gamma)\bar{b}b$ events at the Tevatron, with a $\bar{b}b$ invariant mass peaked at M_{Z_2} in excess of QCD backgrounds if $M_{Z_2} \lesssim 200$ GeV. Here we use Z_2 to denote the mass eigenstate of the heavy Z boson after $Z - Z'$ mixing. Z_2 interference effects may be observable in $e^+e^- \rightarrow \bar{b}b(\bar{c}c)$ at LEP 1.5 energies.

Our work has a distinct vantage point from other recent Z' analyses of the $R_{b,c}$ data that advocate a Z' boson with mass ≈ 1 TeV[9,10] to account for an excess above QCD of the inclusive jet cross section at $E_T > 200$ GeV reported by CDF[19]. Although quark distributions are well constrained by deep inelastic scattering data[20], a smooth rise in the E_T jet cross section compared to QCD expectations can possibly be explained by other means, such as a modification of the gluon structure function at high x [21] or a flattening of $\alpha_s(Q^2)$ at high Q^2 due to new particles[22]. Also the CDF high E_T jet anomaly is not present in preliminary D0 data[23].

A large class of string models with supersymmetry contain additional $U(1)'$ symmetries and additional exotic matter multiplets. In many of these models the Z' and exotic masses are either of $\mathcal{O}(M_Z)$ or of order 10^8 to 10^{14} GeV[24]. Consequently a search for Z' bosons in the electroweak mass region $\lesssim 1$ TeV is well motivated. Through the mixing of the Z'

*The values in the Spring 1996 preliminary update[4] are slightly closer to the SM, deviating by 3.5σ (-1.8σ).

boson with the Z , the predictions of electroweak observables are modified[25,26,27,28]. Thus, it is natural to see if Z, Z' mixing effects can better account for the precision electroweak measurements. In general, this mixing affects both lepton and quark partial widths of the Z as well as the total width. The changes in the widths vary from model to model because of the different chiral couplings. In the usual models based on grand unification with $SO(10)$ or E_6 gauge groups (without kinetic mixing[29]), all Z partial widths are modified. However, because the leptonic widths agree well with SM predictions, an overall fit to the electroweak data is then not significantly improved by Z' mixing in these models and the R_b excess is not explained.

If, however, we consider a model in which the Z' couples solely or dominantly to quarks with a universal strength, a substantial improvement results in the description of the precision electroweak data, as detailed below, and found in other recent analyses[7,9,10,11,16]. A reasonable fit to the data is obtained for a range of universal chiral couplings of the Z' boson. A gauge symmetry generated by baryon number, $U(1)_B$, is an interesting possibility[12], since this avoids potential problems associated with the breaking of global baryon number by quantum gravity effects (e.g., an unacceptable proton decay rate in supersymmetric theories). In this case the Z' has vector couplings. Another possibility is kinetic mixing of the two $U(1)$'s[11,29] to suppress the leptonic couplings. The $U(1)_\eta$ model of E_6 is an interesting model in which this may occur[11]. Here the cancellation of contributions to the Z -leptonic width is fine tuned and leptonic Z_2 decays may still be present at a suppressed level. In the following, we will consider family-universal couplings to baryon and axial-baryon number. As in Refs. [9,10], we assume that the model can be embedded in an anomaly-free theory. Extension of the results to models (such as $U(1)_\eta$) with different couplings to charge $2/3$ and $-1/3$ quarks, or to the family non-universal case, is straightforward.

A Z' coupled to quarks has very interesting implications for physics at the Tevatron collider. If its mass is $\lesssim 200$ GeV, it could be produced in the s -channel and in conjunction with the W , Z or γ and detected via its $Z_2 \rightarrow b\bar{b}$ decay mode (and possibly also through $Z_2 \rightarrow c\bar{c}$). The signatures for WZ_2 and ZZ_2 production would be similar to Higgs boson production WH and ZH , with $H \rightarrow b\bar{b}$ decays, but the Z_2 signals could be considerably higher.

$Z - Z'$ mixing

Following the notation of Ref. [30], the Lagrangian describing the neutral current gauge interactions of the standard electroweak $SU(2) \times U(1)$ and extra $U(1)$'s is given by

$$-\mathcal{L}_{\text{NC}} = eJ_{\text{em}}^\mu A_\mu + \sum_{\alpha=1}^n g_\alpha J_\alpha^\mu Z_{\alpha\mu}^0, \quad (2)$$

where Z_1^0 is the SM Z boson and Z_α^0 with $\alpha \geq 2$ are the extra Z bosons in the weak-eigenstate basis[31]. In our case, we only consider one extra Z_2^0 mixing with the SM Z_1^0 boson. The coupling constant g_1 is the SM coupling $g/\cos\theta_w$. For grand unified theories (GUT) g_2 is related to g_1 by

$$\frac{g_2}{g_1} = \left(\frac{5}{3}x_w\lambda\right)^{1/2} \simeq 0.62\lambda^{1/2}, \quad (3)$$

where $x_w = \sin^2\theta_w$ and θ_w is the weak mixing angle. The factor λ depends on the symmetry breaking pattern and the fermion sector of the theory but is usually of order unity.

Since we only consider the mixing of Z_1^0 and Z_2^0 we can rewrite the Lagrangian in Eq. (2) with only the Z_1^0 and Z_2^0 interactions

$$-\mathcal{L}_{Z_1^0 Z_2^0} = g_1 Z_{1\mu}^0 \left[\frac{1}{2} \sum_i \bar{\psi}_i \gamma^\mu (g_v^{i(1)} - g_a^{i(1)} \gamma^5) \psi_i \right] + g_2 Z_{2\mu}^0 \left[\frac{1}{2} \sum_i \bar{\psi}_i \gamma^\mu (g_v^{i(2)} - g_a^{i(2)} \gamma^5) \psi_i \right], \quad (4)$$

where for both quarks and leptons

$$g_v^{i(1)} = T_{3L}^i - 2x_w Q_i, \quad g_a^{i(1)} = T_{3L}^i, \quad (5)$$

and we consider the case in which Z_2 couples only to quarks,

$$g_v^{q(2)} = \epsilon_V, \quad g_a^{q(2)} = \epsilon_A, \quad g_v^{\ell(2)} = g_a^{\ell(2)} = 0. \quad (6)$$

Here T_{3L}^i and Q_i are, respectively, the third component of the weak isospin and the electric charge of the fermion i ; ϵ_V and ϵ_A are parameters of the Z_2 sector. The mixing of the weak eigenstates Z_1^0 and Z_2^0 to form mass eigenstates Z_1 and Z_2 can be parametrized by a mixing angle θ

$$\begin{pmatrix} Z_1 \\ Z_2 \end{pmatrix} = \begin{pmatrix} \cos\theta & \sin\theta \\ -\sin\theta & \cos\theta \end{pmatrix} \begin{pmatrix} Z_1^0 \\ Z_2^0 \end{pmatrix}. \quad (7)$$

The mass of Z_1 is $M_{Z_1} = 91.19$ GeV and M_{Z_2} is unknown.

Substituting Eq. (7) into Eq. (4) we obtain the interactions of the mass eigenstates Z_1 and Z_2 with fermions

$$- \mathcal{L}_{Z_1 Z_2} = \sum_i \frac{g_1}{2} \left[Z_{1\mu} \bar{\psi}_i \gamma^\mu (v_s^i - a_s^i \gamma^5) \psi_i + Z_{2\mu} \bar{\psi}_i \gamma^\mu (v_n^i - a_n^i \gamma^5) \psi_i \right], \quad (8)$$

where

$$v_s^i = g_v^{i(1)} + \frac{g_2}{g_1} \theta g_v^{i(2)}, \quad a_s^i = g_a^{i(1)} + \frac{g_2}{g_1} \theta g_a^{i(2)}, \quad (9)$$

$$v_n^i = \frac{g_2}{g_1} g_v^{i(2)} - \theta g_v^{i(1)}, \quad a_n^i = \frac{g_2}{g_1} g_a^{i(2)} - \theta g_a^{i(1)}. \quad (10)$$

Here we use the valid approximation $\cos \theta \approx 1$ and $\sin \theta \approx \theta$. The Feynman rules for the interactions of Z_1 and Z_2 with the fermions can be easily obtained from Eq. (8).

Precision Electroweak Constraints

From studies of Z' mixing effects on the Z_1 coupling, the products $\theta \lambda^{1/2} \epsilon_V$ and $\theta \lambda^{1/2} \epsilon_A$ can be determined. Without loss of generality we can take the ϵ_V and ϵ_A to be normalized to unity and write

$$\epsilon_V = \sin \gamma, \quad \epsilon_A = \cos \gamma, \quad \kappa = -\theta \left(\frac{5}{3} x_w \lambda \right)^{1/2}. \quad (11)$$

The partial widths for Z_1 -decays to quarks are determined by the couplings

$$v_s^b = -\frac{1}{2} + \frac{2}{3} x_w - \kappa \sin \gamma = -0.35 - \kappa \sin \gamma, \quad (12)$$

$$a_s^b = -\frac{1}{2} - \kappa \cos \gamma = -0.5 - \kappa \cos \gamma, \quad (13)$$

$$v_s^c = \frac{1}{2} - \frac{4}{3} x_w - \kappa \sin \gamma = 0.19 - \kappa \sin \gamma, \quad (14)$$

$$a_s^c = \frac{1}{2} - \kappa \cos \gamma = 0.5 - \kappa \cos \gamma, \quad (15)$$

where the value $x_w = 0.23$ is used in the approximate equalities. The modifications in the SM partial widths are then

$$\delta\Gamma(Z \rightarrow b\bar{b}) \simeq \kappa C(M_{Z_1}^2) \Gamma^0 (0.69 \sin \gamma + 1.0 \cos \gamma), \quad (16)$$

$$\delta\Gamma(Z \rightarrow c\bar{c}) \simeq -\kappa C(M_{Z_1}^2) \Gamma^0 (0.39 \sin \gamma + 1.0 \cos \gamma), \quad (17)$$

where

$$\Gamma^0 \equiv \frac{G_F M_{Z_1}^3}{2\sqrt{2}\pi} \quad (18)$$

and

$$C(Q^2) = 1 + \frac{\alpha_s}{\pi} + 1.409 \frac{\alpha_s^2}{\pi^2} - 12.77 \frac{\alpha_s^3}{\pi^3}, \quad (19)$$

with $\alpha_s = \alpha_s(Q^2)$ [2]. Fermion mass corrections, effects related to the shift induced in M_Z by the mixing[30], and electroweak corrections are not displayed for simplicity but are incorporated in the numerical analysis.

Similar results apply for the other $T_3 = -1/2$ and $1/2$ flavors, respectively. The total hadronic width

$$\Gamma(Z \rightarrow \text{hadrons}) = 3\Gamma(Z \rightarrow b\bar{b}) + 2\Gamma(Z \rightarrow c\bar{c}) \quad (20)$$

is modified by

$$\delta\Gamma_{\text{had}} = \kappa C\Gamma^0(1.3 \sin \gamma + 1.0 \cos \gamma). \quad (21)$$

Thus, a vector baryonic Z' ($\lambda = \pi/2$) gives the modifications

$$\delta\Gamma(Z \rightarrow b\bar{b}) \simeq 0.69\kappa C\Gamma^0, \quad \delta\Gamma(Z \rightarrow c\bar{c}) \simeq -0.39\kappa C\Gamma^0, \quad \delta\Gamma_{\text{had}} \simeq 1.3\kappa C\Gamma^0. \quad (22)$$

The $Z \rightarrow b\bar{b}$ partial width is increased (for $\kappa > 0$) and the $Z \rightarrow c\bar{c}$ partial width is decreased, which are the directions of the deviations from SM predictions indicated by the LEP data. The increase in the total hadronic width can be compensated by a smaller value of $\alpha_s(M_Z^2)$ in $C(M_{Z_1}^2)$ than that obtained in the SM fits; then both Γ_{had} and Γ_{tot} measurements are well described by the Z' mixing model.

An axial baryonic Z' ($\gamma = 0$) gives the changes

$$\delta\Gamma(Z \rightarrow b\bar{b}) \simeq 1.0\kappa C\Gamma^0, \quad \delta\Gamma(Z \rightarrow c\bar{c}) \simeq -1.0\kappa C\Gamma^0, \quad \delta\Gamma_{\text{had}} \simeq 1.0\kappa C\Gamma^0. \quad (23)$$

Here the effects in the $b\bar{b}$ and $c\bar{c}$ channels are again in the desired direction (for $\kappa > 0$), but larger, and the change in $\delta\Gamma_{\text{had}}$ is somewhat less. A range of γ values can produce fits that are significantly better than the SM; we focus on $\gamma = 0$ and $\pi/2$ henceforth as representative cases. Even better fits could be obtained by adjusting γ . We will also briefly consider the fine-tuned case $\cot \gamma = -1.3$, for which the direct contribution to $\delta\Gamma_{\text{had}}$ vanishes.

We have made fits to the full set of electroweak measurements similar to analyses of the SM[2]. In particular, we include the (important) constraints from deep inelastic neutrino scattering and atomic parity violation, which were not included in the analyses of Refs. [9,10,11]. The best fit value of $\alpha_s(M_Z^2)$ comes out somewhat low for the pure axial and pure vector cases, so we made subsequent fits with $\alpha_s(M_Z^2)$ fixed at 0.11, 0.115, and 0.12. The chi-square for the axial model is moderately increased by fixing α_s at the higher values, while for the vector model the quality of the fit decreases significantly. The values[†] for α_s , m_t , $\theta\lambda^{1/2}$ and M_2/M_1 are listed in Tables 1 and 2. Table 3 contains the results of the model with $\cot\gamma = -1.3$. Excellent fits are obtained with α_s close to the SM fit value $\alpha_s = 0.123$. For comparison with the χ^2 values in these fits, the χ^2 value found in the SM fit is $\chi^2 = 192$ for 208 degrees of freedom. Table 4 compares the fit to the interesting observables R_b , R_c , R_ℓ , Γ_{had} , Γ_{tot} and $A_{\text{FB}}(b\bar{b})$, where the latter quantity is the $b\bar{b}$ asymmetry; the “pull” of each of these observables in the fit is given.

Table 1: Parameters determined by electroweak data analysis for $\gamma = 0$ (Z' with pure axial vector coupling). The χ^2 values are for 206 (207) degrees of freedom for α_s free (fixed). The upper bounds on M_2/M_1 are one sigma mass limits.

$\sin^2\theta_w$	α_s	m_t	$\theta\lambda^{1/2}$	M_2/M_1	χ^2
0.2313(2)	0.095(8)	183_{-11}^{+7}	-0.025(7)	<1.9	176
0.2314(2)	0.11 fixed	181_{-10}^{+7}	-0.014(3)	<2.9	179
0.2315(2)	0.115 fixed	180_{-9}^{+7}	-0.011(3)	<3.9	182
0.2315(2)	0.12 fixed	179_{-9}^{+7}	-0.007(3)	<6.3	185

In the SM fit the Higgs mass is constrained to the range

$$60 < m_H < 100 \tag{24}$$

with the best fit at the lower end of the allowed range. This is driven mainly by R_b and the SLD polarization asymmetry[2]. In the mixing models the preference for any particular

[†]The shifts in the Z_1 couplings depend only on the combination $\theta\lambda^{1/2}$. The shift in M_{Z_1} and the effects of Z_2 exchange have different dependences on λ and θ . However, the global fit results are insensitive to λ in the range 0.25–4 except for the scaling of θ as $\lambda^{-1/2}$. The fit results are given for $\lambda = 1$.

Table 2: Parameters determined by electroweak data analysis for $\gamma = \pi/2$ (Z' with pure vector couplings).

$\sin^2 \theta_w$	α_s	m_t	$\theta\lambda^{1/2}$	M_2/M_1	χ^2
0.2313(2)	0.068(17)	181(7)	-0.037(11)	<1.02	179
0.2315(2)	0.11 fixed	179(7)	-0.010(2)	<1.1	186
0.2315(2)	0.115 fixed	179(7)	-0.007(2)	<1.15	187
0.2315(2)	0.12 fixed	179(7)	-0.004(2)	<1.4	189

Higgs mass value is weakened significantly, especially for the cases which come close to the experimental R_b . Our precision electroweak analysis does not include the case of an approximate Z_2, Z mass degeneracy[32], since the LEP/SLD extractions of the Z -parameters assume a single resonance description. Values of $M_{Z_2} < M_{Z_1}$ area also possible, but we have not analyzed this case in detail.

Table 3: Parameters determined for the model with no direct contribution to $\delta\Gamma_{\text{had}}$ ($\cot \gamma = -1.3$). The standard model fit parameters are also shown. The χ^2 are for 206 (208) degrees of freedom.

	$\sin^2 \theta_w$	α_s	m_t	$\theta\lambda^{1/2}$	M_2/M_1	χ^2
$\delta\Gamma_{\text{had}} = 0$	0.2312(2)	0.121(4)	185_{-8}^{+7}	-0.043(11)	< 1.2	177
SM	0.2315(2)	0.123(4)	180(7)	—	—	192

Z_2 Decays

The decay width of $Z_2(Z_1) \rightarrow f\bar{f}$ is given by

$$\Gamma(Z_{2(1)} \rightarrow f\bar{f}) = \frac{G_F M_{Z_1}^2}{6\pi\sqrt{2}} N_c C(M_{Z_{2(1)}}^2) M_{Z_{2(1)}} \sqrt{1-4x} \left[v_{n(s)}^{f2}(1+2x) + a_{n(s)}^{f2}(1-4x) \right], \quad (25)$$

where $x = m_f^2/M_{Z_{2(1)}}^2$, $N_c = 3$ or 1 if f is a quark or a lepton, respectively, G_F is the Fermi coupling constant, and $M_{Z_1}^0$ is the SM Z mass. We calculated $\alpha_s(M_{Z_2})$ from the two-loop expression with $\Lambda_{\text{QCD}} = 200$ MeV and 5 flavors for $M_{Z_2} < 2m_t$ and 6 flavors above $2m_t$.

Table 4: Comparison of fits to the observables R_b , R_c , R_ℓ , Γ_{had} , Γ_{tot} and $A_{\text{FB}}(b\bar{b})$. (Γ_{had} is actually a quantity derived from the standard fit variables[1,2].) For the vector and axial cases, the results are for $\alpha_s = 0.110$. Widths are in GeV. For each fit the “pull”, i.e., (fit value – expt. value)/error, is shown in square brackets.

	Baryonic Z' Model				
	Expt. (LEP+SLD)	SM	$\gamma = 0$ (axial)	$\gamma = \pi/2$ (vector)	$\cot \gamma = -1.3$ ($\delta\Gamma_{\text{had}} = 0$)
R_b	0.2219(17)	0.2155 [-3.8]	0.2194 [-1.5]	0.2170 [-2.9]	0.2210 [-0.5]
R_c	0.1540(74)	0.172 [2.4]	0.166 [1.6]	0.170 [2.2]	0.164 [1.4]
R_ℓ	20.788(32)	20.77 [-0.6]	20.79 [0.1]	20.78 [-0.3]	20.78 [-0.3]
Γ_{had}	1.7448(30)	1.746 [0.4]	1.747 [0.7]	1.747 [0.7]	1.744 [-0.3]
Γ_{tot}	2.4963(32)	2.500 [1.2]	2.501 [1.5]	2.500 [1.2]	2.497 [0.2]
$A_{\text{FB}}(b\bar{b})$	0.0997(31)	0.102 [0.7]	0.102 [0.7]	0.102 [0.7]	0.100 [0.1]

The Z_2 width is proportional to λ , which sets the strength of the Z_2 coupling; see Eq. (3). For $\lambda = 1$ the total Z_2 width is

$$\Gamma_{Z_2}/M_{Z_2} = 0.022 \quad \text{for } M_{Z_2} < 2m_t, \quad \Gamma_{Z_2}/M_{Z_2} = 0.026 \quad \text{for } M_{Z_2} > 2m_t. \quad (26)$$

The widths would be increased somewhat if there are open channels for decay into superpartners or exotic particles.

Z_2 Production in the s -channel

The Z_2 state can be directly produced at a hadron collider via the $q\bar{q} \rightarrow Z_2$ subprocesses, for which the cross section in the narrow Z_2 width approximation is[33]

$$\hat{\sigma}(q\bar{q} \rightarrow Z_2) = K \frac{2\pi G_F M_{Z_1}^2}{3\sqrt{2}} [(v_n^q)^2 + (a_n^q)^2] \delta(\hat{s} - M_{Z_2}^2). \quad (27)$$

The K -factor represents the enhancement from higher order QCD processes, estimated to be[33] $K = 1 + \frac{\alpha_s(M_{Z_2}^2)}{2\pi} \frac{4}{3} \left(1 + \frac{4}{3}\pi^2\right) \simeq 1.3$. In the approximation that the terms proportional to θ in the couplings v_n^q , a_n^q are neglected,

$$(v_n^q)^2 + (a_n^q)^2 = (0.62)^2 \lambda \quad (28)$$

and the cross section is independent of the parameter γ .

The jet-jet invariant mass resolution smearing of hadron collider detectors is typically $\Delta m(jj)/m(jj) = 0.1$, which includes the effects of QCD radiation and detector smearing. Since this mass resolution well exceeds the Z_2 width when the Z_2 is $\mathcal{O}(M_Z)$, we include a Gaussian smearing of $m(jj)$ with this rms resolution in calculating $m(jj)$ distributions associated with Z_2 decays.

In calculating the QCD background to s -channel Z_2 production we include interference effects and calculate the $q\bar{q} \rightarrow q\bar{q}$ process at the amplitude level, including Z_2 , Z and γ exchanges along with the QCD gluon exchange amplitudes. The non-interfering backgrounds from the W -exchange processes $q\bar{q}' \rightarrow q\bar{q}'$ and $q\bar{q}' \rightarrow q'\bar{q}$ and the backgrounds from gg , gq , and $g\bar{q}$ initiated processes are added to get the full jet-jet cross section. In our calculations we use the CTEQ3L parton distributions of Ref. [34].

The UA2 Collaboration[35] has detected the $W + Z$ signal in the dijet mass region $48 < m(jj) < 138$ GeV and has placed upper bounds on $\sigma B(Z_2 \rightarrow jj)$ over the range $80 < m(jj) < 320$ GeV. Figure 1 compares our Z_2 model predictions for $\lambda = 0.2, 0.6$, and 1 with the UA2 upper bounds. We see that a λ upper bound of order 0.7 to 1 is indicated for $100 < M_{Z_2} < 180$ GeV. However, because of the uncertainty in the K -factor in the theoretical cross section calculation and the difficulty in obtaining an experimental bound by subtraction of a smooth background, we subsequently consider $\lambda = 1$ at any M_{Z_2} for illustration.

Inclusive Z_2 production with $Z_2 \rightarrow b\bar{b}$ decays may be detectable at the Tevatron as an excess of events in the $b\bar{b}$ invariant mass distribution at $m(b\bar{b}) \approx M_{Z_2}$ and in the inclusive transverse momentum distribution of the b , which has a Jacobian peak at $p_T(b) \simeq \frac{1}{2}M_{Z_2}$. These distributions are illustrated for leading order QCD in Fig. 2. Vertex and semileptonic tagging of the b 's can be used to reject the backgrounds from other quarks and gluons. The backgrounds due to $gg \rightarrow b\bar{b}$ production are nonetheless very large, so identification of the signal contribution here is difficult.

The Z_2 can be produced in e^+e^- collisions via any direct e^+e^- coupling and its e^+e^- coupling induced by mixing. Here we consider the e^+e^- coupling that results solely from mixing. Figure 3 illustrates the effects of a $M_{Z_2} = 105$ GeV resonance on the $e^+e^- \rightarrow b\bar{b}$ and

$c\bar{c}$ cross sections and on the $e^+e^- \rightarrow \bar{b}b$ forward-backward asymmetry A_{FB} . An interference of Z_2 , Z_1 and γ contributions gives the wave-like structure, with the interference vanishing close to $\sqrt{s} = M_{Z_2}$. The signs of the interference contributions are opposite in $\bar{b}b$ and $c\bar{c}$ (and are related at $\sqrt{s} < M_{Z_2}$ to the signs of the deviations of R_b and R_c from the SM). Consequently, flavor identification is necessary to observe the effect. To quantify the effect, we take the difference of cross-sections at ± 1 GeV on either side of the interference zero. In the $M_{Z_2} = 105$ GeV illustration the values of $\Delta\sigma = \sigma(\sqrt{s} = 104 \text{ GeV}) - \sigma(\sqrt{s} = 106 \text{ GeV})$ are

$$\begin{aligned} \Delta\sigma_{\bar{b}b}^{SM+Z_2(axial)} &= 39 \text{ pb}; & \Delta\sigma_{\bar{b}b}^{SM+Z_2(vector)} &= 34 \text{ pb}; & \Delta\sigma_{\bar{b}b}^{SM} &= 22 \text{ pb}; \\ \Delta\sigma_{c\bar{c}}^{SM+Z_2(axial)} &= 0.72 \text{ pb}; & \Delta\sigma_{c\bar{c}}^{SM+Z_2(vector)} &= 11 \text{ pb}; & \Delta\sigma_{c\bar{c}}^{SM} &= 18 \text{ pb}. \end{aligned} \quad (29)$$

A fine energy scan at LEP 1.5 in the region of $\sqrt{s} = M_{Z_2}$ could measure these Z_2 resonance effects.

Vector Boson Pair Production

In the SM, W^+W^- and WZ pair production can provide stringent tests of the gauge theory since there are large cancellations between a s -channel gauge boson amplitude and a t -channel fermion exchange amplitude. For example, consider $p\bar{p} \rightarrow WZ + \text{anything}$ production at $\sqrt{s} = 1.8$ TeV. The components of the cross section are

$$\sigma(W^*) = 16 \text{ pb}, \quad \sigma(f) = 20 \text{ pb}, \quad \sigma(W^*, f) = -34 \text{ pb}, \quad \sigma_{\text{total}} = 2 \text{ pb}, \quad (30)$$

where W^* denotes the s -channel resonance, f the fermion exchange contribution, and (W^*, f) the interference contribution. This cancellation is mandated by the asymptotic s -dependence of the cross section[33]. In the case of WZ_2 or ZZ_2 pair production the s -channel boson contributions are highly suppressed by the mixing angle θ . Consequently, we expect much larger pair production cross sections than in the SM when M_{Z_2} is of order M_Z . Because the Z' couplings to quarks are universal, there is no reason for a cancellation of s - and t -channel contributions[36].

The cross sections at the Tevatron energy $\sqrt{s} = 1.8$ TeV are shown for $\lambda = 1$ in Fig. 4. We have included a K -factor of $K = 1.3$ to approximate next-to-leading order QCD contributions[37]. The cross sections for WZ_2 , Z_1Z_2 , and γZ_2 scale linearly with λ .

For comparison the corresponding SM cross sections for WZ_1 , γZ_1 and Z_1Z_1 are indicated by squares on the figure. We have imposed the acceptance $p_T(\gamma) > 15$ GeV and $|\eta(\gamma)| < 1$ on the final state photon.

The prospects for detecting the Z_2 would be best in the $Z_2 \rightarrow b\bar{b}$ final state, with b -tagging by vertex detector or semileptonic decays to reject backgrounds from light quarks and gluons in the $(\gamma, W, Z)jj$ final state. The $b\bar{b}$ branching fraction of Z_2 is

$$B(Z_2 \rightarrow b\bar{b}) = 0.2. \quad (31)$$

The signature of WZ_2 with $Z_2 \rightarrow b\bar{b}$ are the same as those for Higgs searches in WH and ZH final states with $H \rightarrow b\bar{b}$ decays. Figure 5 compares the $(W, Z, \gamma)b\bar{b}$ cross sections for $\lambda = 1$ with $(W, Z)H \rightarrow b\bar{b}$, where $B(H \rightarrow b\bar{b}) \approx 1$ for the mass range shown. We have included a K -factor of $K = 1.25$ to approximate the next-to-leading order QCD contributions[38] to WH and ZH cross sections here. We see that for $M_{Z_2} \approx 105$ GeV the $W + (Z_2 \rightarrow b\bar{b})$ cross section with $\lambda = 1$ is a factor 3 times the $W + (H \rightarrow b\bar{b})$ cross section. Other experimentally interesting channels include $Z_1 + (Z_2 \rightarrow b\bar{b})$ and $\gamma + (Z_2 \rightarrow b\bar{b})$, whose cross sections are also given in Fig. 5. The Z_1Z_2 and Z_2Z_2 cross sections will give $b\bar{b}b\bar{b}$, $b\bar{b}c\bar{c}$, $c\bar{c}c\bar{c}$ events above the SM QCD predictions.

The backgrounds to the $(\gamma, W, Z)Z_2$ signals in the $Z_2 \rightarrow b\bar{b}$ channels arise from the $(\gamma, W, Z)g^*$ final states with a virtual gluon g^* giving a $b\bar{b}$ pair. For the calculation of $p\bar{p} \rightarrow Wb\bar{b}$ we used the formulas in Ref. [39], while we used MADGRAPH [40] to calculate $p\bar{p} \rightarrow Zb\bar{b}$ and $p\bar{p} \rightarrow \gamma b\bar{b}$. The differential cross sections $d\sigma/dm(b\bar{b})$ for the signals and backgrounds are shown in Figs. 6, 7, and 8 for $Wb\bar{b}$, $Zb\bar{b}$, and $\gamma b\bar{b}$ final states, respectively. While the background is a continuum in the $m(b\bar{b})$ spectrum, the signal gives a peak around the Z_2 mass. In Figs. 6(a), 7(a), and 8, the solid histogram is the SM background, while the long-dashed and short-dashed histograms show the effect of the additional Z_2 boson of mass 105 GeV and 85 GeV, respectively. Figure 6(b) and 7(b) show the corresponding signals and backgrounds for the SM Higgs boson of the same mass as the Z_2 . Since the Z_2 is universally coupled, the cross sections for $c\bar{c}$ final states are the same as for $b\bar{b}$. If the UA2 bound of $\lambda \lesssim 1$ were weakened, larger Z_2 cross sections would be obtained with larger λ values.

In Table 5 we present estimates of the number of $Z_2 \rightarrow b\bar{b}$ signal and $b\bar{b}$ background

Table 5: Expected $Z_2 \rightarrow b\bar{b}$ signals and background event rates at the Tevatron with 100 pb^{-1} luminosity and 100% detection efficiency, for $\Delta m(b\bar{b}) = \pm 10 \text{ GeV}$ centered on $M_{Z_2} = 105 \text{ GeV}$. A Z_2 coupling $\lambda = 1$ is assumed. The event numbers in parentheses are for acceptance cuts $p_T(b), p_T(\bar{b}) > 10 \text{ GeV}$, $|\eta(b)|, |\eta(\bar{b})| < 2$, $|\cos\theta^*| < 2/3$, where θ^* is the angle of the b with respect to the beam in the $b\bar{b}$ rest frame.

	Signal	Background
s -channel Z_2	6×10^4 (3×10^4)	1.3×10^7 (6×10^5)
WZ_2 (with $W \rightarrow e\nu, \mu\nu$)	9.6	6.1
Z_1Z_2 (with $Z_1 \rightarrow \nu\bar{\nu}$)	3.3	4.9
Z_1Z_2 (with $Z_1 \rightarrow e\bar{e}, \mu\bar{\mu}$)	1.1	1.7
γZ_2	80	120

events that would be expected at the Tevatron in an invariant mass bin $\Delta m(b\bar{b}) = \pm 10 \text{ GeV}$ centered on $M_{Z_2} = 105 \text{ GeV}$, assuming 100 pb^{-1} luminosity and 100% detection efficiency. The signal event rates are at the interesting level for Z_2 discovery.

Summary

In summary, we have shown the following:

- A Z' boson with baryonic couplings improves the overall fit to precision electroweak observables, including LEP and SLD measurements along with other low-energy measurements such as neutrino scattering. Our conclusion in this regard is in agreement with other recent analyses which were based on Z -pole observables only.
- The precision electroweak analysis constrains the product $\theta\lambda^{1/2}$ of the Z, Z' mixing angle θ and the overall Z' coupling strength $\lambda^{1/2}$.
- The electroweak analysis favors a light Z_2 mass, $M_{Z_2} \lesssim 200 \text{ GeV}$. Values of M_{Z_2} below the Z -mass are not ruled out.

- The s -channel production rate of Z_2 in $p\bar{p}$ collisions is constrained by UA2 dijet measurements, with couplings up to $\lambda \sim 1$ allowed.
- The Z_2 can be produced in association with γ, W, Z , with cross sections at the Tevatron exceeding corresponding cross sections for Z_1 production in association with γ, W, Z .
- The $Z_2 \rightarrow b\bar{b}$ decay mode is an important signal for Z_2 production in association with γ, W, Z at the Tevatron, giving a resonant enhancement in the $b\bar{b}$ invariant mass spectrum above the QCD background. These processes have a better signal-to-background ratio than the s -channel process.
- The Z_2 causes interference effects in $e^+e^- \rightarrow b\bar{b}(\bar{c}c)$ that may be observable at LEP 1.5. The interference contribution changes sign for \sqrt{s} near M_{Z_2} and is correlated with the signs of the deviations of $R_b(R_c)$ from SM predictions.

Acknowledgments

One of us (V.B.) thanks D. Amidei, D. Carlsmith, T. Han, J. Huston, W.-Y. Keung, and P. Mercadante for discussions. This research was initiated at the Institute for Theoretical Physics at Santa Barbara, whose support is gratefully acknowledged. This research was supported in part by the U.S. Department of Energy under Grants No. DE-FG02-95ER40896, No. DE-FG03-93ER40757, and No. DOE-EY-76-02-3071, in part by the National Science Foundation Grant No. PHY94-07194, and in part by the University of Wisconsin Research Committee with funds granted by the Wisconsin Alumni Research Foundation.

References

- [1] The LEP Collaborations ALEPH, DELPHI, L3, OPAL and the LEP Electroweak Working Group, CERN-PRE/95-172; P.B. Renton, plenary talk at Int. Conf. on High Energy Physics, Beijing (1995).

- [2] J. Erler and P. Langacker, Phys. Rev. **D52**, 441 (1995) and “Standard Model of Electroweak Interactions”, in the 1995 off-year partial update of the 1996 edition of the PDG (available at <http://pdg.lbl.gov>); P. Langacker, hep-ph/9511207.
- [3] K. Hagiwara, hep-ph/9512425 and hep-ph/9601222.
- [4] LEP Electroweak Working Group, LEPEWWG/96-01.
- [5] A. Djouadi et al., Nucl. Phys. **B349**, 48 (1991); M. Bouwens and D. Finnell, Phys. Rev. **D44**, 2054 (1991); G.L. Kane, R.G. Stuart, and J.D. Wells, Phys. Lett. **B354**, 350 (1995); P.H. Chankowski and S. Pokorski, Phys. Lett. **B356**, 307 (1995) and hep-ph/9509207; X. Wang, J. Lopez, and D. Nanopoulos, Phys. Rev. **D52**, 4116 (1995); S. Mrenna and C.-P. Yuan, Phys. Lett. **B367**, 188 (1996); C.E.M. Wagner, hep-ph/9510341; J.L. Feng, N. Polonsky, and S. Thomas, hep-ph/9511324; Y. Yamada, K. Hagiwara, and S. Matsumoto, hep-ph/9512227; J. Ellis, J. Lopez, and D. Nanopoulos, hep-ph/9512288; A. Brignole, F. Feruglio, and F. Zwirner, hep-ph/9601293; J.L. Feng, H. Murayama, and J.D. Wells, hep-ph/9601295; E. Simmons and Y. Su, hep-ph/9602267; P.H. Chankowski and S. Pokorski, hep-ph/9603310.
- [6] E. Ma and D. Ng, hep-ph/9505268; E. Ma, Phys. Rev. **D53**, 2276 (1996); G. Bhattacharyya, G.C. Branco, and W.-S. Hou, hep-ph/9512239; T. Yoshikawa, hep-ph/9512251; M. Carena, H.E. Haber, and C.E.M. Wagner, hep-ph/9512446; C.-H. V. Chang, D. Chang, and W.-Y. Keung, hep-ph/9601326; P.G. Hung, hep-ph/9604271.
- [7] V. Barger and P. Langacker, October 1995 (unpublished).
- [8] Y. Zhang and B.L. Young, Phys. Rev. **D51**, 6584 (1995); B. Holdom and M.V. Ramana, Phys. Lett. **B365**, 309 (1996).
- [9] P. Chiappetta, J. Layssac, F.M. Renard, C. Verzegnassi, hep-ph/9601306.
- [10] G. Altarelli, N. Di Bartolomeo, F. Feruglio, R. Gatto, and M. Mangano, hep-ph/9601324.

- [11] K.S. Babu, C. Kolda, J. March-Russell, hep-ph/9603212.
- [12] C.D. Carone and H. Murayama, Phys. Rev. **D52**, 4159 (1995); Phys. Rev. Lett. **14**, 322 (1995); D. Bailey and S. Davidson, Phys. Lett. **B348**, 185 (1995).
- [13] E. Malwaki, T. Tait, and C.-P. Yuan, hep-ph/9603349 (1996); D.J. Muller and S. Nandi, hep-ph/9602390.
- [14] A. Leike, S. Riemann, and T. Riemann, Phys. Lett. **B291**, 187 (1992); A. Kundu, hep-ph/9504417; T. Gehrman and W.T. Stirling, hep-ph/9603380.
- [15] P. Frampton and B. Wright, hep-ph/9604260.
- [16] K. Agashe, M. Graesser, I. Hinchliffe, and M. Suzuki, hep-ph/9604266.
- [17] G.-H. Wu, hep-ph/9508376; E.H. Simmons, R.S. Chivukula, and J. Terning, hep-ph/9509392; C.-X. Yue, Y.-P. Kuang, and G.-R. Lu, hep-ph/9509412; N. Kitazawa, hep-ph/9510334; N. Kitazawa and T. Yanagida, hep-ph/9511364.
- [18] D. Garcia and J. Sola, Phys. Lett. **B357**, 349 (1995); D. Cornelli, hep-ph/9505439; J.K. Kim, Y.G. Kim, J.S. Lee, and K.Y. Lee, hep-ph/9509319; P. Bamert, hep-ph/9512445; H. Zheng, hep-ph/9602340; P. Bamert, C.P. Burgess, J.M. Cline, D. London, and E. Nardi, hep-ph/9602438; D. Cornelli and J.P. Silva, hep-ph/9603221; M. Masip and A. Rasin, Nucl. Phys. **B460**, 449 (1996); D. Atwood, L. Reina, and A. Soni, hep-ph/9603210; J.S. Lee and J.K. Kim, hep-ph/9603225.
- [19] CDF Collaboration, F. Abe et al., FERMILAB-PUB-96/020-E (1996).
- [20] E.W.N. Glover, A.D. Martin, R.G. Rogers and W.J. Stirling, hep-ph/9603327; E.W.N. Glover, talk presented at *Pheno96* Symposium, Madison, Wisconsin, April 1–3, 1996.
- [21] J. Huston, E. Kovacs, S. Kuhlmann, H.L. Lai, J.F. Owens, D. Soper, W.K. Tung, hep-ph/9511386.
- [22] V. Barger, M.S. Berger, and R.J.N. Phillips, University of Wisconsin preprint MADPH-95-920 (hep-ph/9512325); P. Kraus and F. Wilczek, hep-ph/9601279.

- [23] H. Schullmann, talk at *Pheno96* Symposium, Madison, Wisconsin, April 1–3, 1996.
- [24] M. Cvetič and P. Langacker, hep-ph/9511378 and 9602424.
- [25] P. Langacker, R. Robinett, and J. Rosner, Phys. Rev. **D30**, 1470 (1984); J. Rosner, Phys. Rev. **D35**, 2244 (1987).
- [26] V. Barger, N.G. Deshpande, and K. Whisnant, Phys. Rev. Lett. **56**, 30 (1986); V. Barger, N.G. Deshpande, J.L. Rosner, and K. Whisnant, Phys. Rev. **D35**, 2893 (1987).
- [27] L.S. Durkin and P. Langacker, Phys. Lett. **166B**, 436 (1986); U. Amaldi et al., Phys. Rev. **D36**, 1385 (1987).
- [28] J.L. Hewett and T.G. Rizzo, Phys. Rep. **183**, 193 (1989).
- [29] B. Holdom, Phys. Lett. **B259**, 329 (1991).
- [30] P. Langacker and M.-X. Luo, Phys. Rev. **D45**, 278 (1992).
- [31] For a recent review on Z' gauge bosons see M. Cvetič and S. Godfrey, UPR-648-T, hep-ph/9504216, summary of the Working Subgroup on Extra Gauge Bosons of the DPF long-range planning study, in *Electroweak Symmetry Breaking and Beyond the Standard Model*, eds. T. Barklow, S. Dawson, H. Haber, and J. Seigrist (World Scientific 1995).
- [32] F. Caravaglios and G.G. Ross, Phys. Lett. **B346**, 159 (1995).
- [33] V. Barger and R.J.N. Phillips, *Collider Physics* (Addison-Wesley, 1987).
- [34] H.L. Lai *et al.* (CTEQ Collaboration), Phys. Rev. **D51**, 4763 (1995).
- [35] UA2 Collaboration, J. Alitti et al., Z. Phys. **C49**, 17 (1991).
- [36] M. Cvetič and P. Langacker, Phys. Rev. **D46**, 4943 (1992); T. Rizzo, Phys. Rev. **D47**, 956 (1993); M. Cvetič, P. Langacker, and J. Liu, Phys. Rev. **D49**, 2405 (1994).
- [37] J. Ohnemus, Phys. Rev. **D47**, 940 (1993); **D50**, 1931 (1994); U. Baur, T. Han, and J. Ohnemus, Phys. Rev. **D51**, 3381 (1995).

- [38] T. Han and S. Willenbrock, Phys. Lett. **B273**, 167 (1990); J. Ohnemus and W.J. Stirling, Phys. Rev. **D47**, 2722 (1993); A. Stange, W. Marciano, and S. Willenbrock, Phys. Rev. **D49**, 1354 (1994).
- [39] Z. Kunszt, Nucl. Phys. **B247**, 339 (1984).
- [40] T. Stelzer and W. Long. Comput. Phys. Commun. **81**, 357 (1994).

Figures

1. The total cross section for the production of $p\bar{p} \rightarrow Z_2 \rightarrow jj$ at $\sqrt{s} = 630$ GeV for $\lambda = 0.3, 0.6, 1$. The UA2 90% CL upper limit on the production of a heavy boson decaying into 2 jets is shown.
2. The $b\bar{b}$ invariant mass distribution and the inclusive $p_T(b)$ distribution at the Tevatron, including the contribution of a Z_2 resonance, with $M_{Z_2} = 105$ GeV and $\lambda = 1$. The solid histogram denotes the SM background, including the $Z_1 \rightarrow b\bar{b}$ contribution. The dashed histogram includes the Z_2 contribution. The histograms at the bottoms of the figure are the Z_2 contributions alone. The acceptance cuts in Table 5 are imposed.
3. The $e^+e^- \rightarrow \bar{b}b(\bar{c}c)$ cross sections and the asymmetry $A_{\text{FB}}(b\bar{b})$ versus \sqrt{s} in the vicinity of a Z_2 resonance of mass $M_{Z_2} = 105$ GeV, with $\lambda = 1$ and $\theta = -0.011$. The solid curve denotes the SM background. The dashed and dot-dashed curves include the contribution of an axial ($\gamma = 0$) and vector ($\gamma = \pi/2$) baryonic Z' , respectively.
4. The total cross sections for the production of $p\bar{p} \rightarrow WZ_2, ZZ_2, Z_2Z_2, \gamma Z_2$ (solid curves) at $\sqrt{s} = 1.8$ TeV. The cross sections for the standard model $WZ, ZZ, \gamma Z$ (squares) and WH, ZH (dashed curves) production are also shown.
5. The cross sections for the production of $p\bar{p} \rightarrow WZ_2, ZZ_2, \gamma Z_2$ followed by $Z_2 \rightarrow b\bar{b}$ (solid curves) at $\sqrt{s} = 1.8$ TeV. The cross sections for the standard model $WZ, ZZ, \gamma Z$ with $Z \rightarrow b\bar{b}$ (squares) and WH, ZH with $H \rightarrow b\bar{b}$ (dashed curves) production are also shown.
6. The $b\bar{b}$ invariant mass distribution $d\sigma/dm(b\bar{b})$ for $Wb\bar{b}$ final state. The solid histogram is the sum of the continuum $Wb\bar{b}$ and the SM Z boson, while the long-dashed and short-dashed histograms show the additional Z_2 boson of mass 105 and 85 GeV, respectively. Part (b) is similar to part (a) with the additional Z_2 replaced by the SM Higgs boson.
7. The $b\bar{b}$ invariant mass distribution $d\sigma/dm(b\bar{b})$ for $Zb\bar{b}$ final state. The solid histogram is the sum of the continuum $Zb\bar{b}$ and the SM Z boson, while the long-dashed and short-

dashed histograms show the additional Z_2 boson of mass 105 and 85 GeV, respectively. Part (b) is similar to part (a) with the additional Z_2 replaced by the SM Higgs boson.

8. The $b\bar{b}$ invariant mass distribution $d\sigma/dm(b\bar{b})$ for $\gamma b\bar{b}$ final state. The solid histogram is the sum of the continuum $\gamma b\bar{b}$ and the SM Z boson, while the long-dashed and short-dashed histograms show the additional Z_2 boson of mass 105 and 85 GeV, respectively.

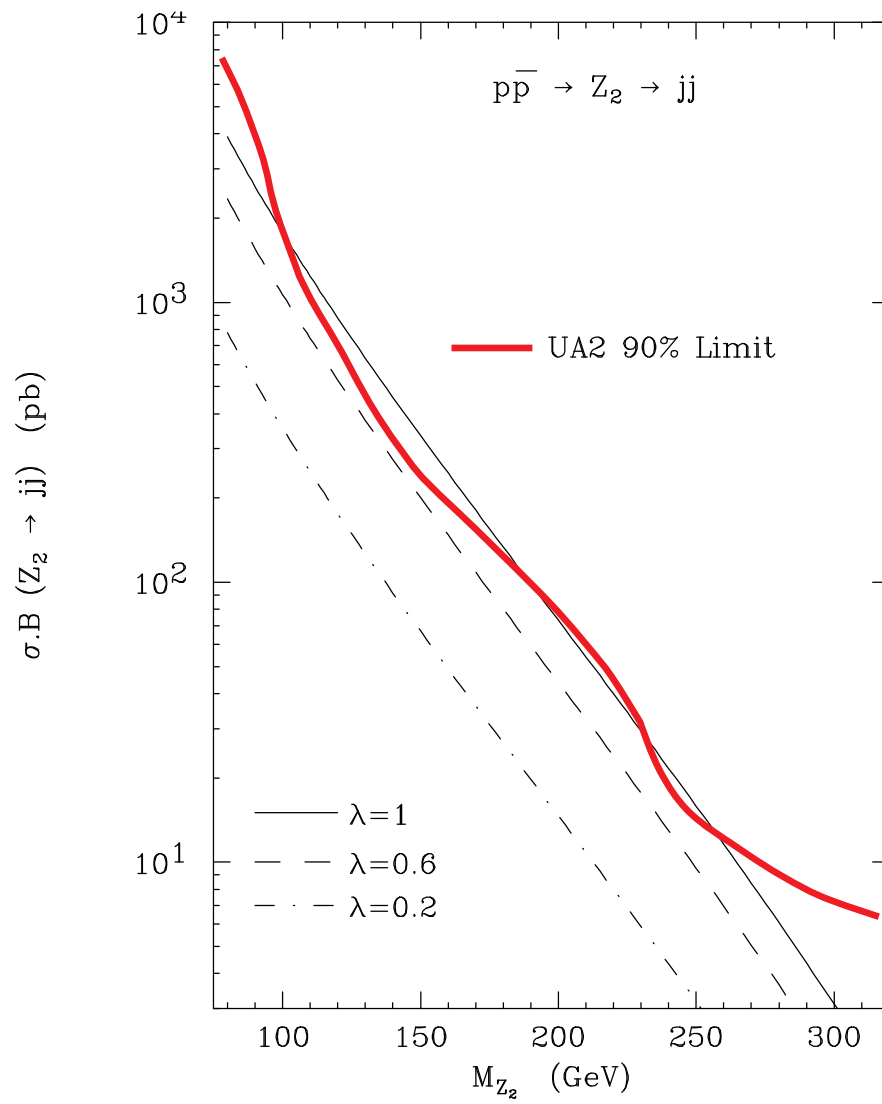


Fig. 1

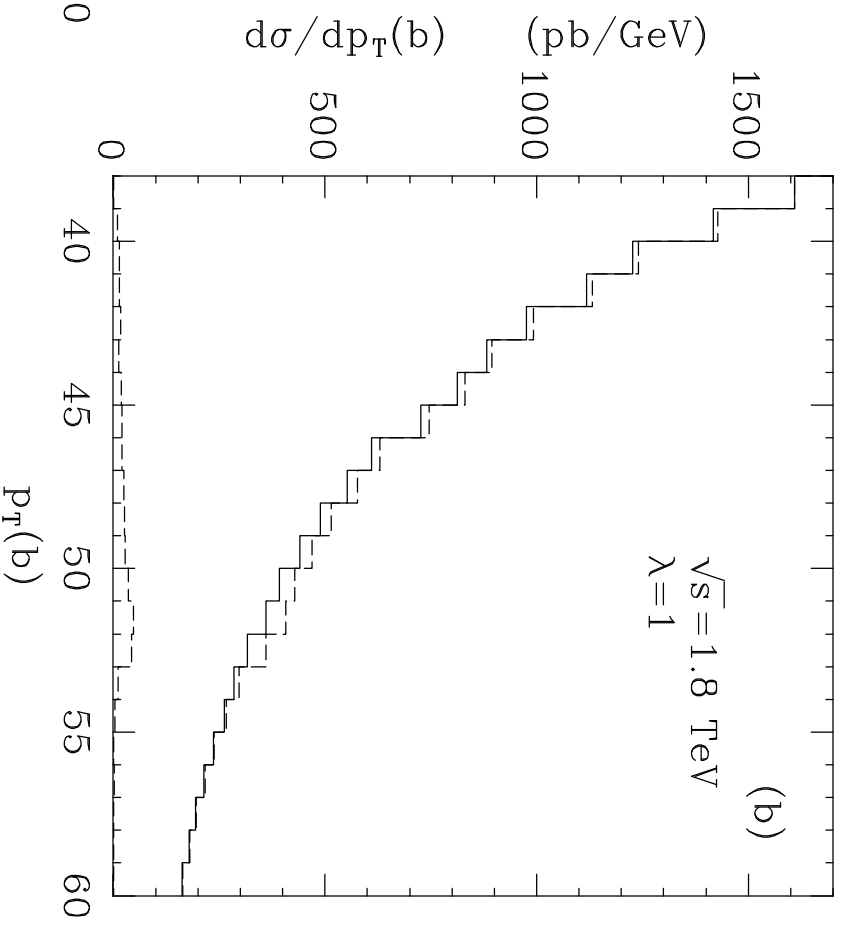
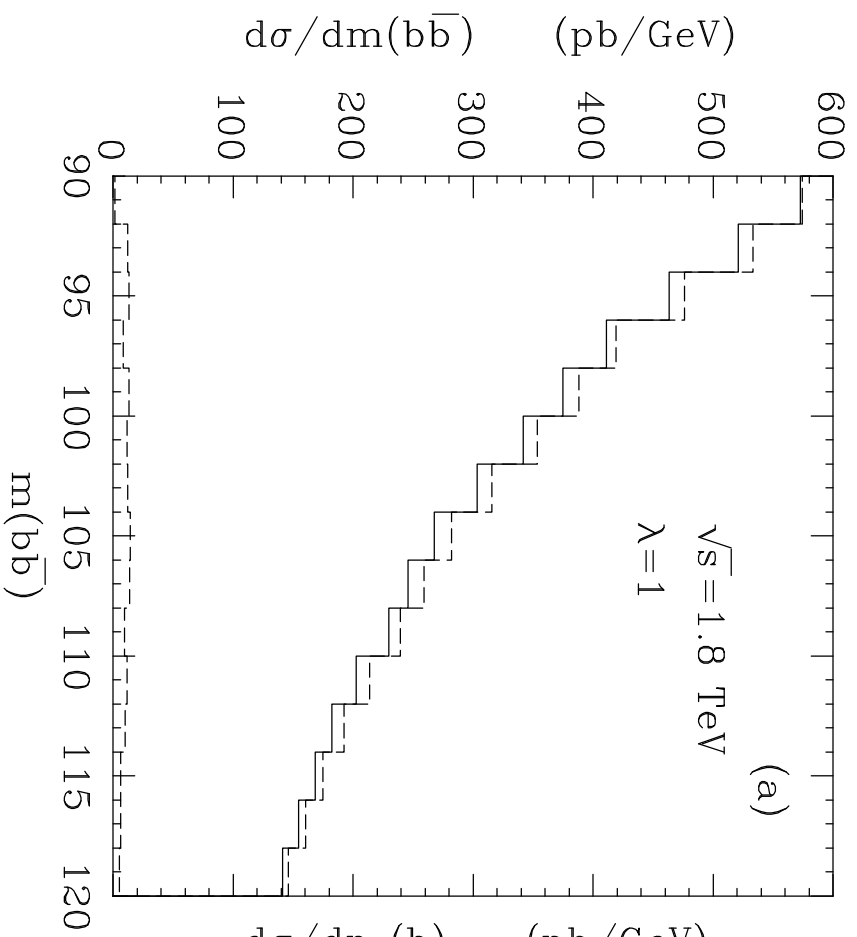


Fig.2

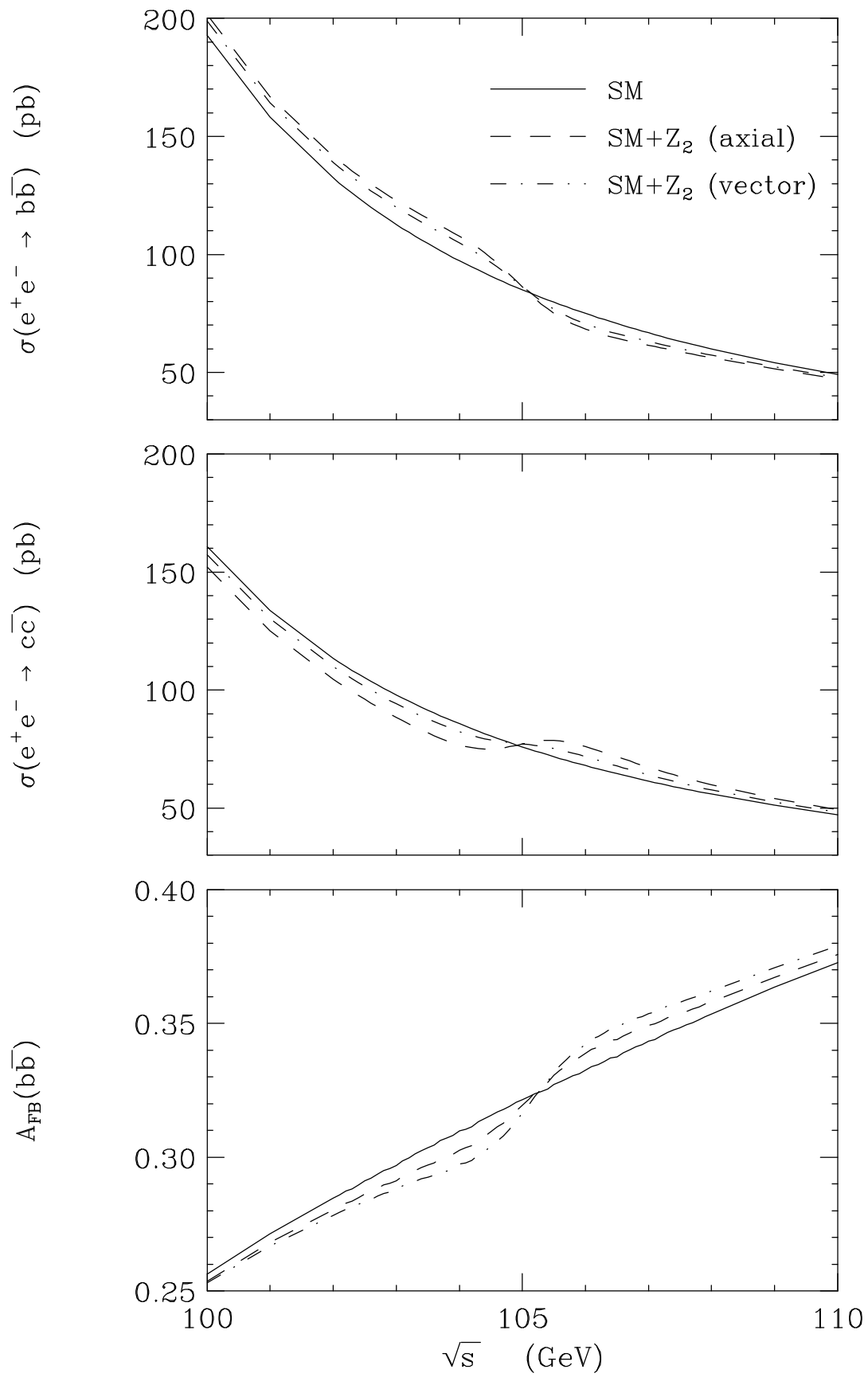


Fig.3

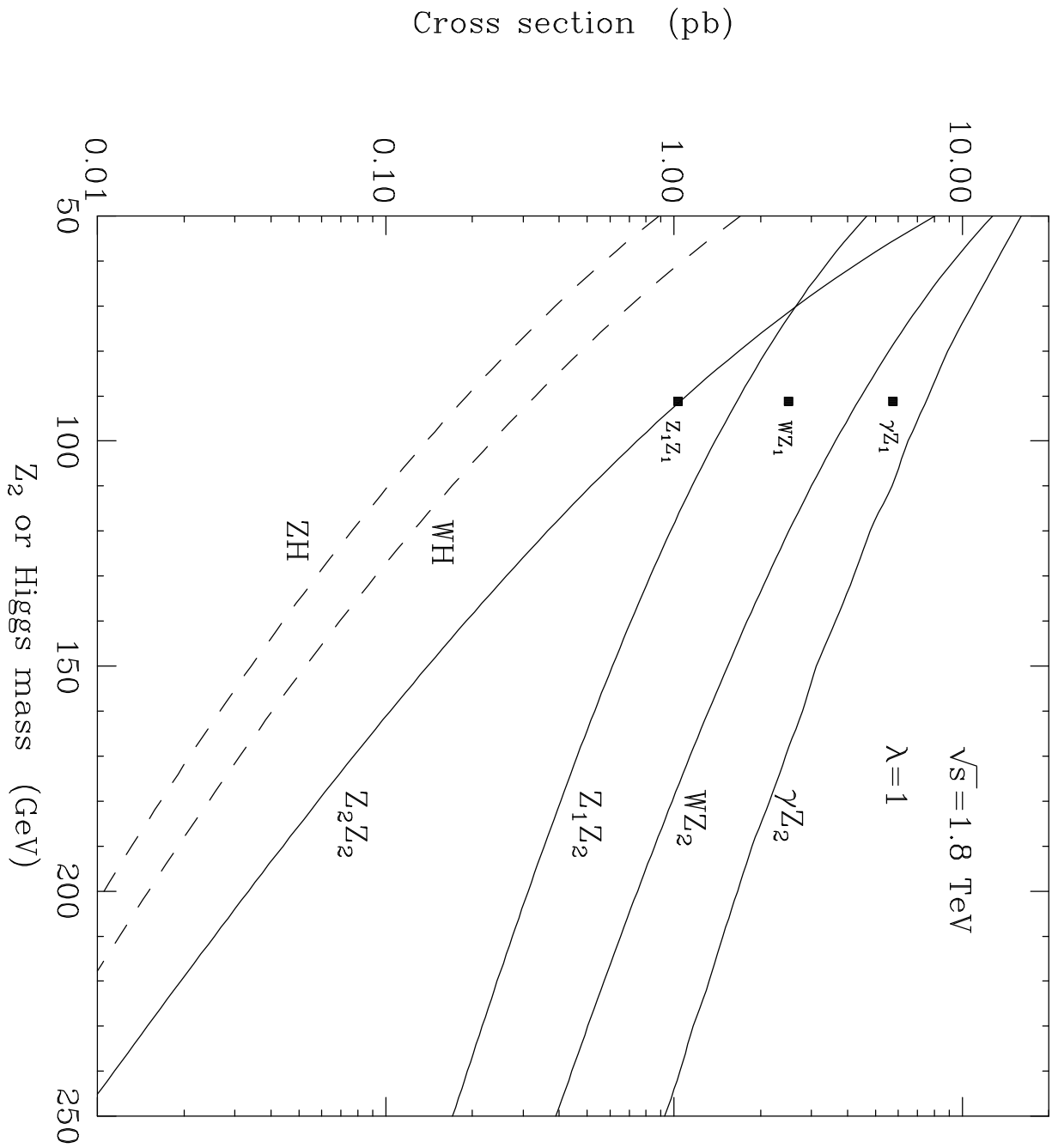


Fig.4

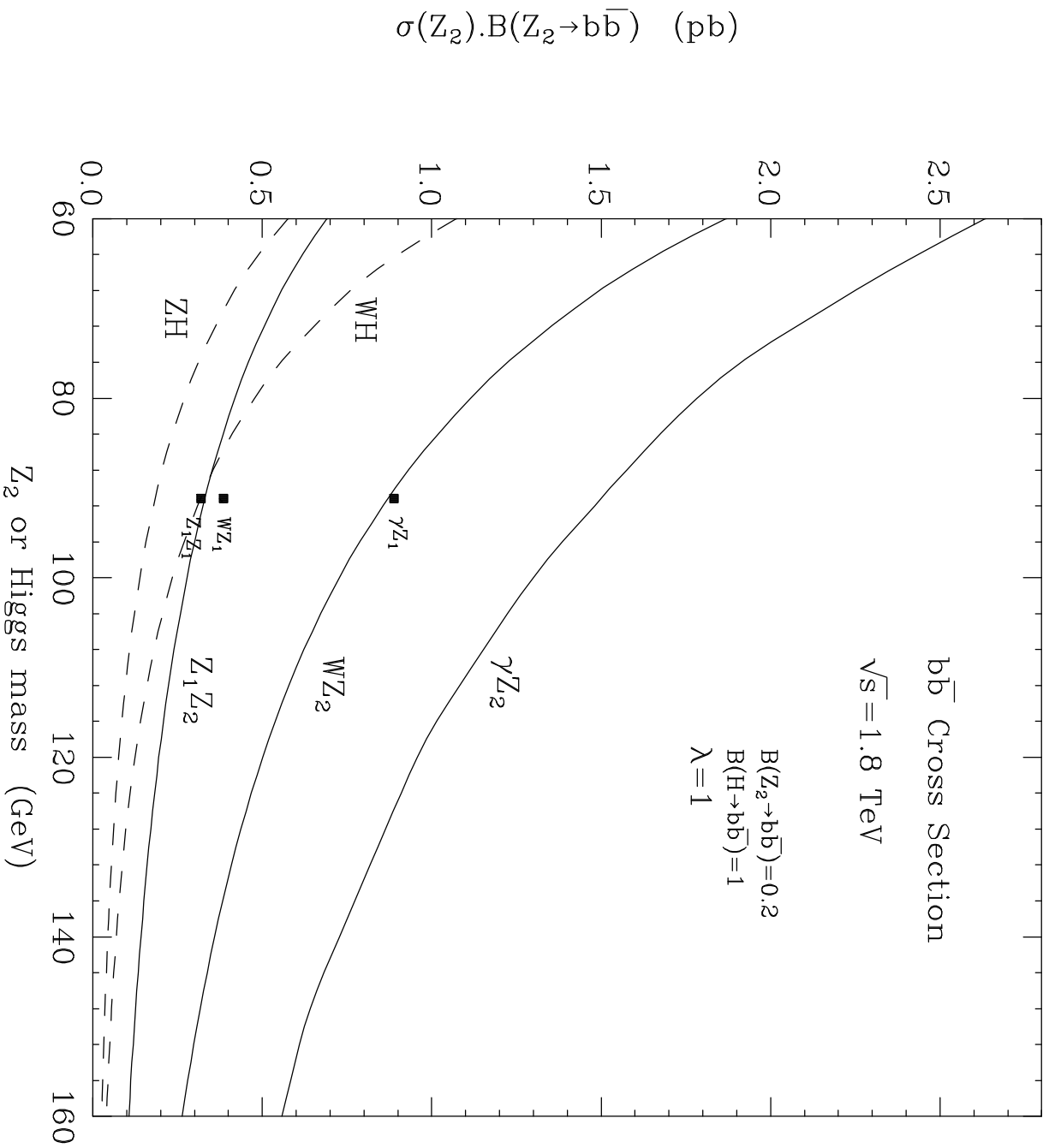


Fig.5

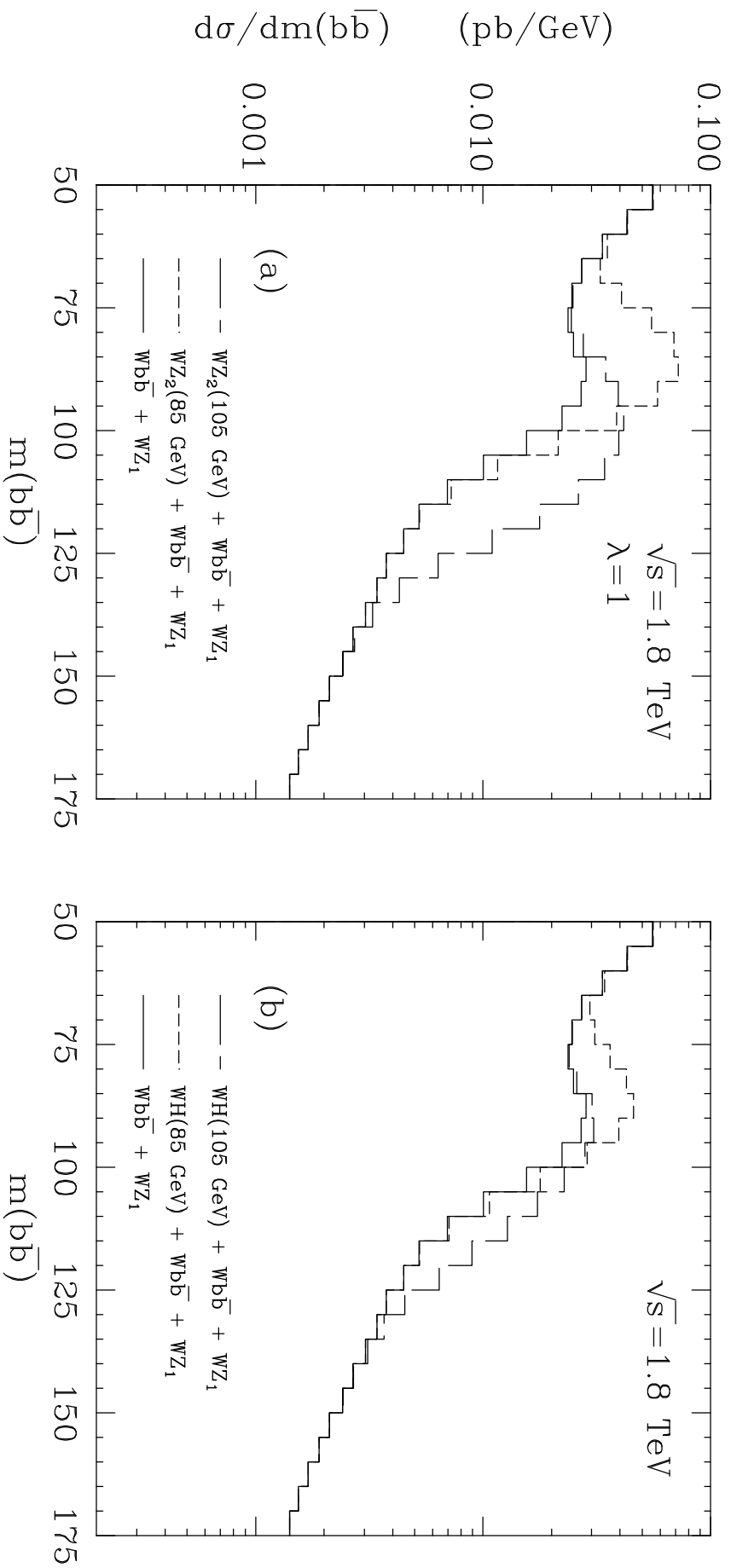


Fig.6

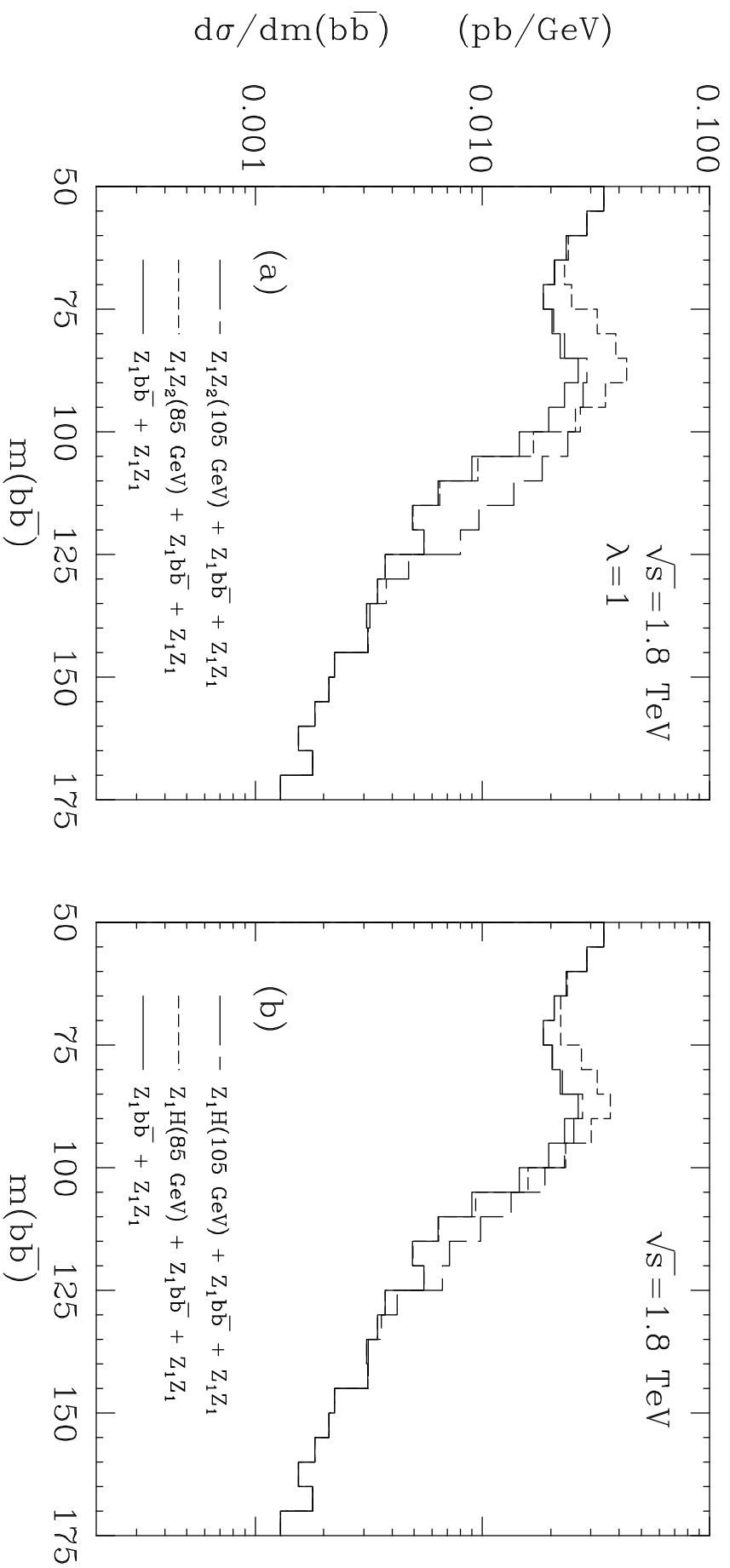


Fig. 7

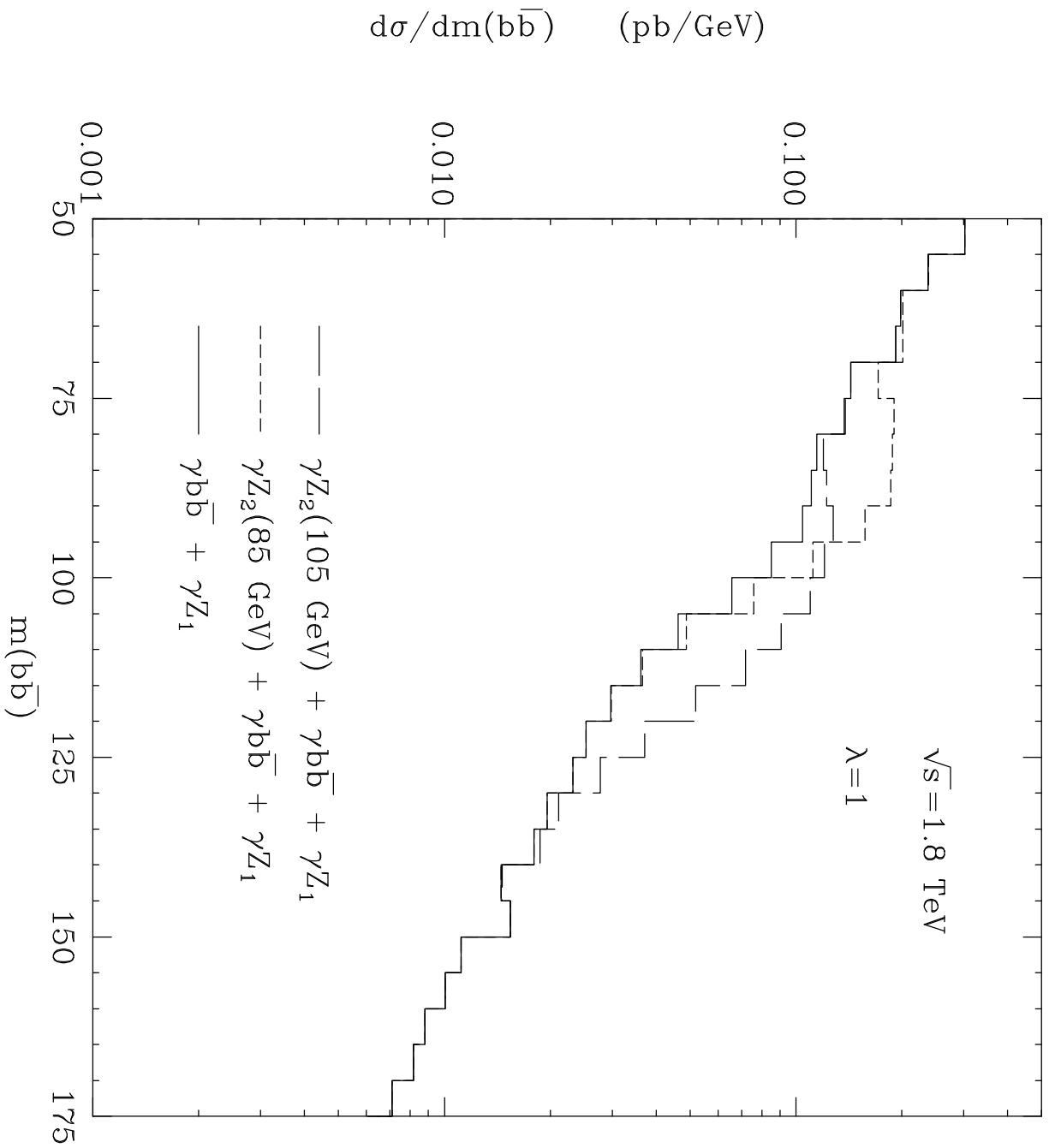


Fig. 8